Technical Report No. 32-636

Total Radiation Heat Transfer Gage for Hypervelocity Shock Tube Experiments

George M. Thomas
Wesley A. Menard

JET PROPULSION LABORATORY
CALIFORNIA INSTITUTE OF TECHNOLOGY
PASADENA, CALIFORNIA
August 1, 1964

Technical Report No. 32-636

Total Radiation Heat Transfer Gage for Hypervelocity Shock Tube Experiments

George M. Thomas
Wesley A. Menard

Bain Dayman, Jr.

Bain Dayman, Jr., *Chief*
Aerodynamic Facilities Section

JET PROPULSION LABORATORY
CALIFORNIA INSTITUTE OF TECHNOLOGY
PASADENA, CALIFORNIA

August 1, 1964

Prepared Under Contract No. NAS 7-100
National Aeronautics & Space Administration

CONTENTS

FIGURES

FIGURES (Cont'd)

ABSTRACT

29007

A heat transfer gage has been developed for measuring the total radiation from shock-heated gases in the spectral region from 0.2 to 2.7 μ. The gage consists essentially of a thin film platinum resistance gage which is coated with a thin carbon film. The requirements for the use of the gage in shock tube experiments are that the absorptance of the carbon film on platinum substrate be essentially constant over the spectral region of interest, and that the response time of the gage be of the order of 1 μsec. This Report describes the theory of operation and the technique of preparing the gages. Measurements of the reflectance of multilayer carbon films are presented. The methods of calibrating the gage and of relating the gage response to the radiance of the radiation source are described in detail. Finally, preliminary shock tube measurements are made using the total radiation gage. These are found to be in good agreement with both theory and experiment.

Author

I. INTRODUCTION

The purpose of this Report is to describe a heat transfer gage which has been developed for measuring the total equilibrium radiative heat transfer to the stagnation point of a flat-faced cylinder. This gage was designed for use in an experimental shock tube investigation of the radiation from planetary atmospheres. The total radiation gage described here consists essentially of a thin film resistance gage coated with a thin layer of carbon of known absorptance. The resistance gage technique has been used previously (Refs. 1, 2) for shock tube investigations of convective heat transfer, etc. Recently (Refs. 3, 4), thin film gages in the form of black body cavities or carbon-coated gages have been employed for total radiation measurements.

The heat transfer gage to be described in this Report has a response time of approximately 1 μsec and is thus suitable for making measurements during the extremely

short test times (10 to 20 μsec) available in high-speed shock tubes. The principle of the gage operation is that radiation incident on the carbon film covering the resistance gage is highly absorbed. This heats the thin film gage backing material, after which the resistance gage responds in its usual fashion. The resistance gage is isolated from the hot shock tube gases by a window which eliminates the thermal heating of the gage and allows for measurement of the radiative heating alone.

This Report is divided into four sections. First, the requirements for the gage and the details of the gage components are discussed. The next section describes theoretical considerations relating the gage response to the actual radiation from the gas volume being viewed by the gage. The third section describes the details of calibrating the gage, and the last section describes the use of the gage in shock tube experiments.

II. TOTAL RADIATION GAGE

The concept of the total radiation measurement is illustrated in Fig. 1. The model is a flat-faced cylinder with a diameter of 1.25 in. The gage is mounted inside the shock tube model behind a pyrex window. The size of the window and the distance of the gage from the window define the field of view of the gage. Photons from the shock layer strike a thin film of carbon covering the resistance gage, and the energy is transformed into heat. The thin film resistance gage then responds to the temperature rise of its backing material.

A. Absorbing Film Requirements

The shock tube requirement of fast response and high sensitivity made a thin-film sensing element the natural choice for the heat transfer gage. Radiation incident on a platinum gage surface would be highly reflected, and the portion absorbed by the film would vary with the wavelength of the incident radiation. It appeared possible, however, to appreciably increase the gage absorptance by covering it with a highly absorbing thin film coating. The coating must be sufficiently thin to allow rapid diffusion of heat to the sensing element in order not to seriously affect the response time.

The second requirement is that the coating must have a reflectance which does not vary with wavelength over the wavelength region of interest. The major contributions to the total radiation from gases in the temperature range considered here are found in the wavelength region from 0.2 to 1.0 μ. This consideration determined the minimum wavelength region for which the gage must exhibit a flat absorptance characteristic.

Carbon films appeared to offer several advantages for this application. The techniques for evaporating carbon films are well known, and the films have the high mechanical strength desirable for gage construction. Previous investigators (Ref. 5) have found that carbon films are highly absorbing and have satisfactory thermal diffusion times.

Evaporated carbon films were prepared under carefully controlled laboratory conditions in order to duplicate film uniformity and thickness as nearly as possible. These films were then mounted over platinum sputtered pyrex samples. Samples containing one, two, and three layers of approximately equal thickness carbon films were then tested for spectral reflectance in the wavelength region from 0.2 to 2.7 μ. The thickness of a single layer of the carbon film placed on the samples was measured to be less than 1 μ. The sputtered platinum film was found to be completely opaque to the incident light, and the absorptance of the carbon film is therefore given by

$$F = 1 - U \tag{1}$$

where F is the fraction of the incident light absorbed, and U is the fractional reflectance measured in the experiment. The results of the measurements are presented in Fig. 2. For comparison purposes, the reflectance of uncoated opaque platinum films and massive

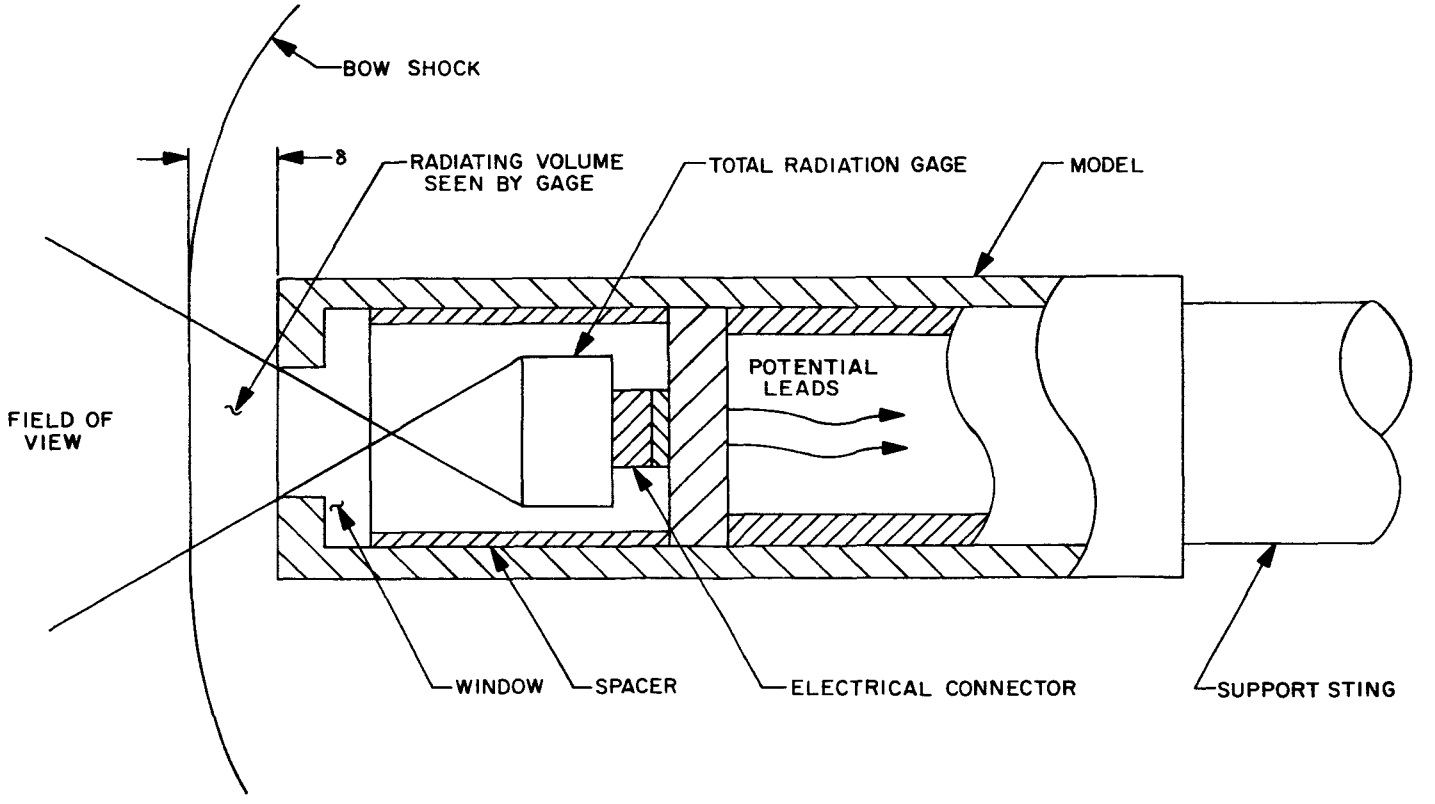

Fig. 1. Schematic of radiation gage model geometry

graphite (Ref. 6) is also presented. The absorptance of all the films is approximately 80% and constant over the wavelength region from 0.2 to 0.7 μ. In this wavelength range, the reflectance is that of *massive graphite*. The results for two- and three-layer films were identical for the entire wavelength region from 0.2 to 2.7 μ and are presented as a single curve. Beyond 0.7 μ, the single-layer films exhibited considerably more variation with wavelength than did the two- and three-layer films. The results indicate that if the bulk of the total radiation being measured lies below 0.7 μ, there is little error in assuming the absorptance to be constant over the entire wavelength region from 0.2 to 2.7 μ. The constant transmission of the pyrex window in the 0.3- to 2.7-μ region determines the wavelength coverage in practice.

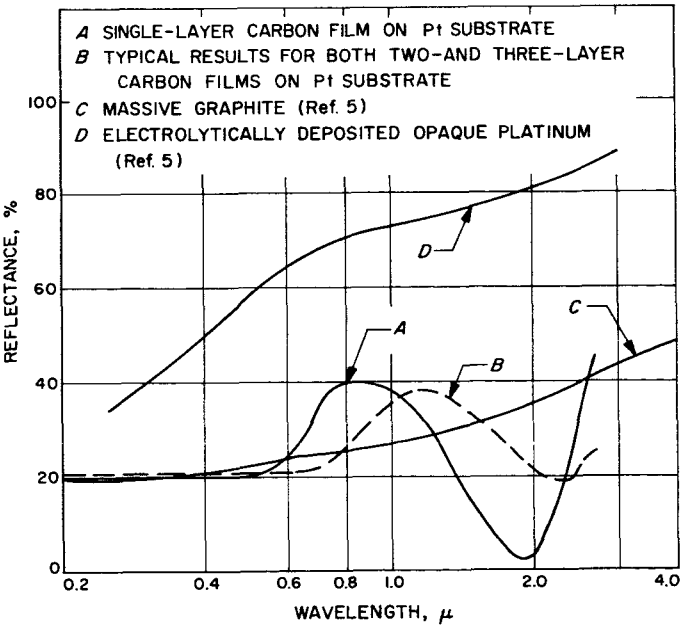

Fig. 2. Specular and diffuse reflectance measurements

B. Response Time

The theoretical model for obtaining the gage response time is illustrated in Fig. 3. The radiant heat flux, $q(t)$, is incident on a slab composed of two materials (1 and 2). The thin film gage measures the surface temperature of

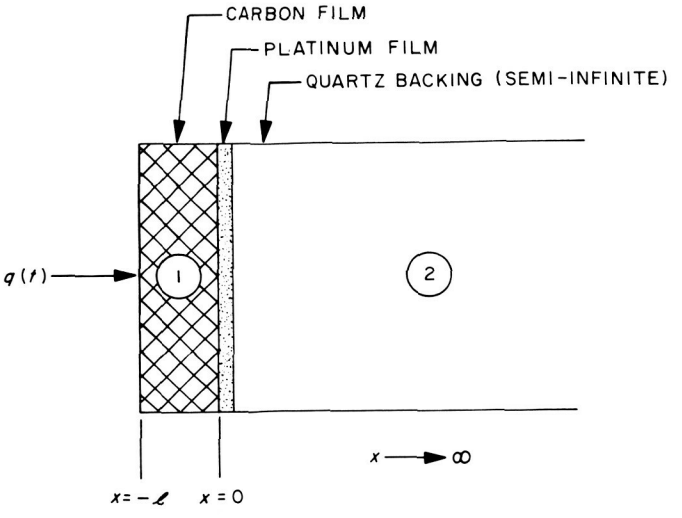

Fig. 3. Theoretical model of the multilayer heat transfer gage

its backing material. For this reason it is necessary to relate the heat transfer, $q(t)$, to the temperature history of the backing material surface. The heat flow may be assumed one-dimensional since the thicknesses of the layers are much less than other characteristic dimensions of the problem (a typical thickness is 1.0 μ for the carbon film and 0.1 μ for the platinum). A second assumption is that the effect of the platinum film may be neglected altogether. This assumption is justified since the characteristic thermal transit time for the platinum film is much less than that for the carbon film.

The solution to the problem outlined above has been given by previous investigators (Ref. 5), and details of the calculation will not be presented here. The results show that the temperature as a function of time of the carbon-quartz interface depends on two parameters:

a. The thermal transit time of Material 1,

$$\tau_1 = \ell^2 \rho_1 C_1 / 4 k_1$$

b. The quantity,

$$\sigma = \sqrt{k_2 \rho_2 C_2 / k_1 \rho_1 C_1}$$

where k_1, ρ_1, and C_1 are the thermal conductivity, density, and heat capacity of Material 1 (carbon), k_2, ρ_2, and C_2 are the same properties of Material 2 (quartz), and ℓ is the thickness of the carbon film. For times much larger than τ_1, the temperature at the interface becomes equal to the temperature (T^*) that the surface of Material 2 would have if Material 1 were removed. The time required to reach the temperature T^* is determined by the value of σ and the type of heat input $q(t)$.

For measurements behind the incident shock wave in a shock tube, the radiation heat transfer, $q(t)$, is a constant during the test time. For $t \gg \tau$, the temperature rise of the interface is given by

$$x = 0 \qquad \Delta T(t) = \frac{2Q}{\sqrt{\pi \rho_2 C_2 k_2}} \sqrt{t} \qquad (2)$$

where $q(t) = Q =$ constant. The temperature response is therefore a parabola. The value of τ_1 for a 5,000 Å carbon film is approximately 2×10^{-8} sec. The value of σ for carbon on quartz shows that the temperature T^* is reached in about 100 τ_1 or about 2 μsec. The theoretical response time of the gage is therefore approximately 2 μsec. The thin film gage voltage response, which will be derived later, has the same time dependence as the temperature response.

C. Gage Construction and Circuit

A completed total radiation gage is shown in Fig. 4. The gage was constructed by sputtering a thin film of platinum (0.035×0.75 in.) along one end of the rectangular quartz backing material. The platinum was then bonded to the quartz by baking in a furnace at 1200°F. Strips of platinum of greater thickness were then sputtered along two opposite sides of the quartz at each end of the film. After rebaking, solder was applied directly over the sputtered sides of the gage, lowering the final resistance to a negligible value compared to the thin film. Two copper wires were then soldered to the sides of the gage, forming a very strong connection to support the gage weight. The loose ends of the two wires were then soldered to the pins of a small electrical connector which serves as the mechanical support for the gage as well as

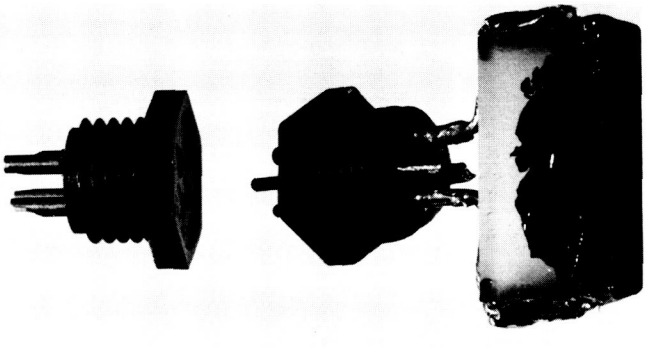

Fig. 4. Total radiation gage

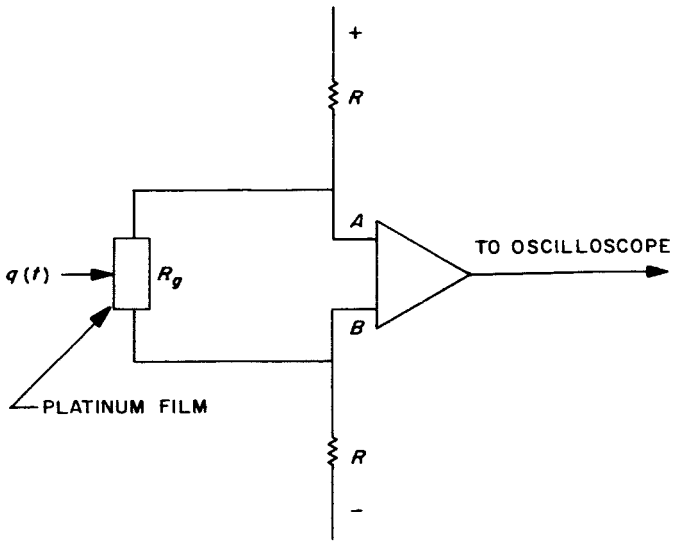

Fig. 5. Schematic of the heat transfer gage circuit

providing a means of removing the gage from the electrical circuit. The final step involved mounting the evaporated carbon film in good thermal contact with the resistance film. Carbon was evaporated onto a standard size pyrex microscope slide. The carbon film was removed from the slide by immersion in a weak solution of potassium hydroxide and distilled water. After removal from the slide, the carbon film floats free on the surface of the solution. The film was then gently lifted from the surface by bringing the gage up from below the surface. After drying, the carbon film was found to form a good mechanical bond with the platinum film. Good thermal contact was also achieved (to be shown later in comparing the theoretical and experimental response times for the gage).

The electrical circuit for the thin film gage is shown in Fig. 5. Power is supplied to the circuit by a 45-v battery. The current limiting resistors (R) are chosen large in comparison to the gage resistance (R_g) in order to maintain a constant current in the gage circuit. A female electrical connector (see Fig. 4) allows insertion of the gage into the circuit. The gage output-voltage leads are connected to a Tektronix Type D differential preamplifier in order to eliminate circuit noise. The output of the amplifier is displayed on an oscilloscope.

III. INTERPRETATION OF GAGE RESPONSE

To make the radiation gage measurement quantitative, the gage response must be related to the intensity of the radiator. Two sources will be considered: 1) an arbitrary volume of gas, and 2) the special case of a plane parallel layer which was chosen for the experimental geometry. A window is considered to be located between the source and detector, since the gage must be isolated from thermal contact with the gas.

The geometry of the problem is illustrated in Fig. 6. The radiation from the gas volume is assumed to be uniform and isotropic. For a transparent and isothermal gas volume, the energy reaching the detector area, dA_i, is given by

$$dq_i\, dA_i = \mu_w\, G_\lambda\, d\lambda\, dV \left(\frac{dA_i \cos\theta}{S_i^2}\right) \qquad (3)$$

where $G_\lambda d\lambda$ is the rate of energy emitted from the volume element dV per unit solid angle in the wavelength interval λ to $\lambda + d\lambda$, μ_w is the constant spectral transmission of a window located between the volume element and the detector surface, and the term in parenthesis is the solid angle. The heat transfer to the area dA_i from the entire volume seen by the elemental area is thus:

$$q_i = \mu_w \overline{G} f_i\,(y) \qquad (4)$$

where

$$\overline{G} = \int G_\lambda\, d\lambda$$

$$f_i\,(y) = \int \frac{dV \cos\theta}{S_i^2}$$

The term $\overline{G}$ is the rate of energy emitted from the gas per unit volume, per unit solid angle, and depends only

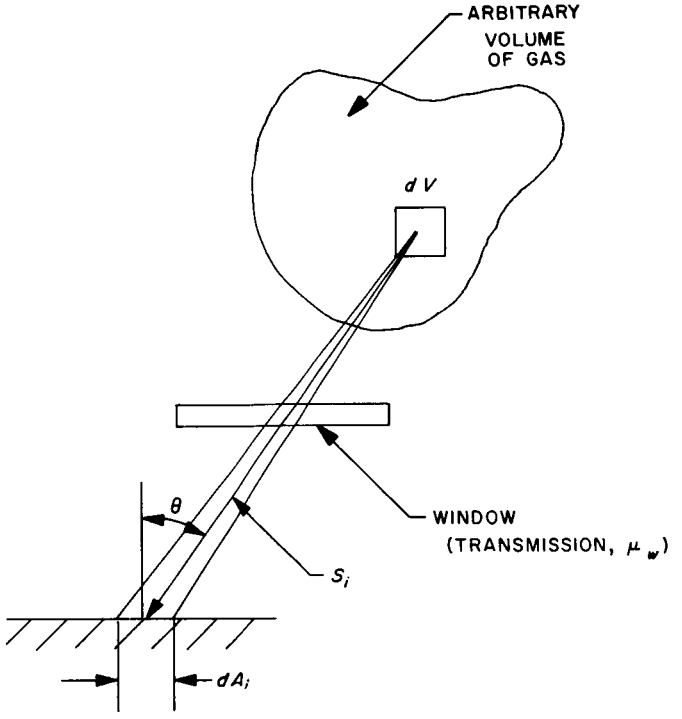

Fig. 6. Geometry of the theoretical model used for calculating the heat flux to a differential element of the gage

on the thermodynamic state of the gas. The term $f_i(y)$ shall hereafter be referred to as the view factor, and is a function only of the geometry of the experiment.

For the case of a detector area located at one surface of a plane parallel, infinite slab of gas, Eq. (3) can be integrated immediately (see Ref. 7) to obtain:

$$q = W\frac{\delta}{2} \tag{5}$$

where $\mu_{ic} = 1$ for the case of no window, $W = 4\pi\bar{G}$ is the gas radiance in w/cm^3, and δ is the thickness of the plane parallel layer. This case corresponds roughly to the stagnation point heat transfer to a flat-faced cylinder with a constant shock layer thickness δ.

In order to relate the gas radiance to the total radiation gage response, the geometry shown in Fig. 7 is considered. The gage is located behind a window with the platinum resistance element parallel to the plane of a circle (the optical stop shown in Fig. 7) located at one surface of a plane parallel gas layer. The heat transfer, q_i, to a differential element, dA_i, of the gage is given by Eq. (4). By assuming that the heat flow is one-dimensional for each differential element of the gage surface, the solution of the one-dimensional heat conduction equation (Eq. 2), may be applied to each element.

$$\Delta T_i = \frac{2}{\beta}\sqrt{t}\, q_i\, F \tag{6}$$

where ΔT_i is the temperature rise of the gage element, F is the absorptance of the gage surface, and $\beta = \sqrt{\pi\rho_2 c_2 k_2}$ is a thermal material property of the quartz. The voltage change of a differential element due to a temperature change, ΔT_i, is given by

$$\Delta E_i = I_0\, \alpha\, r_0\, \Delta T_i\, \Delta y_i \tag{7}$$

where I_0 is the current flowing through the gage, $r_0\Delta y_i$ is the resistance of the element of length Δy_i, and α is the temperature coefficient of resistance of the gage material.

The total voltage change over the entire length of the gage due to the heating is obtained by summing the incremental changes

$$\Delta E = \sum_i \Delta E_i \tag{8}$$

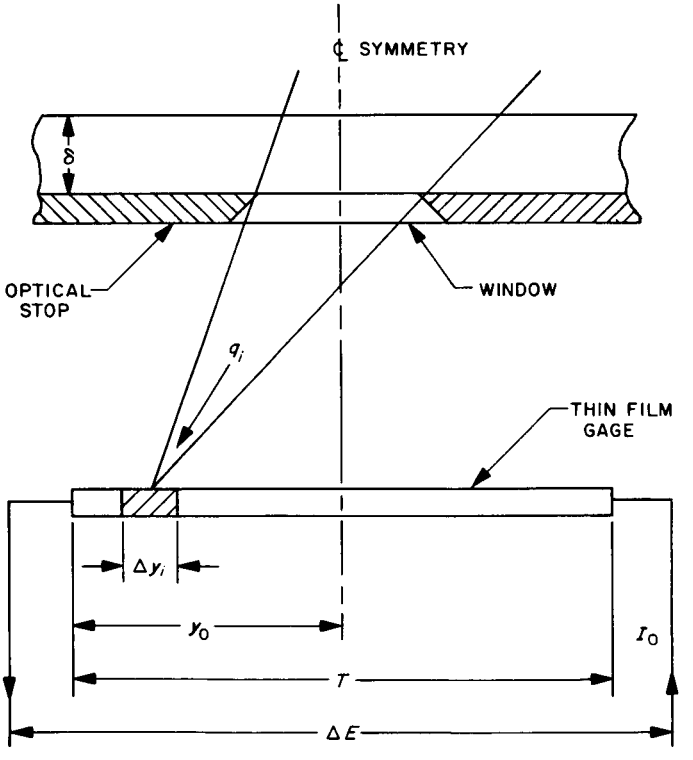

Fig. 7. Theoretical model for relating the gage response to the heat transfer distribution along the gage surface

By combining Eqs. (6), (7), and (8), and converting the sum to an integral the following result is obtained:

$$\frac{\Delta E}{\sqrt{t}} = \frac{4\Phi E_{\circ} F}{L}\int_{\circ}^{y_{\circ}} q\,(y)\,dy \qquad (9)$$

where $\Phi = \alpha/\beta$, $E_{\circ} = I_{\circ} r_{\circ} L$, and L is the length of the gage strip. Equation (9) relates the gage response to the heat transfer distribution along the gage surface. Equation (4) may now be combined with Eq. (9) to relate the gas radiance to the gage response as follows:

$$\frac{\Delta E}{\sqrt{t}} = \left(\frac{\mu_{ir}\, F\, E_{\circ}\, \Phi}{L}\right)\frac{W}{\pi}\int f_i(y)dy \qquad (10)$$

and, letting

$$2\,\xi = L\pi/\mu_{ir}\, F\, E_{\circ}\, \Phi \int f_i(y)dy$$

Eq. (10) may be written as

$$W = 2\,\xi\,\frac{\Delta E}{\sqrt{t}} \qquad (11)$$

The quantity ξ is a constant to be determined for a given total radiation gage, and the necessary measurements to determine the constant will be described in the next section. The quantity $\Delta E/\sqrt{t}$ is obtained from the time history of the gage voltage response to incident radiation from a gas of radiance W.

The heat transfer to the stagnation point of a flat-faced cylinder may be expressed in terms of the gage response by combining Eqs. (5) and (11) to obtain

$$q = \xi\,\frac{\Delta E}{\sqrt{t}}\,\delta \qquad (12)$$

It is a consequence of the analysis to be presented in the Appendix that the view factor term $\int f(y)dy$ is directly proportional to the shock stand-off distance (δ) to a good approximation, and thus that $\xi \approx 1/\delta$. Therefore, Eq. (12) may be written

$$q = \text{const}\,\Delta E/\sqrt{t}$$

This result shows that the stagnation point heat transfer to a flat-faced cylinder may be measured without knowledge of the shock stand-off distance. However, if the gas radiance is to be measured (see Eq. 11), it is necessary to determine δ by measurement or by another means.

IV. CALIBRATION

There are two possible methods for calibrating the heat transfer gage, as shown by Eq. (11), where the radiance was given by

$$W = 2\xi\,\frac{\Delta E}{\sqrt{t}}$$

The first method would be to choose a source of known radiance, and measure the quantity $\Delta E/\sqrt{t}$ for a given gage geometry. This method would determine the quantity ξ and provide an overall calibration of the system as a single unit. Unfortunately, short-duration radiation sources of known radiance and sufficient intensity for calibration are not available. Therefore, a second method was chosen which determines the individual quantities making up ξ. From the preceding section, ξ is given by

$$2\,\xi = L\pi/\mu_{ir}\, F\, E_{\circ}\, \Phi \int f(y)dy$$

The term F is the absorptance of the carbon and is measured according to the description given in Section II.

The window transmission, μ_w, may be measured by the usual photometric technique using a tungsten lamp and monochromator-photomultiplier combination. The measurements of E_0 and L_0 are likewise straightforward. The view factor term $\int f(y)dy$ may be computed theoretically. Details of this calculation are discussed in the Appendix. The method of determining the remaining quantity, Φ, is now considered.

The quantity Φ is given by

$$\Phi = \frac{\alpha}{\sqrt{\pi \rho_2 C_2 k_2}}$$

and is a property of both the platinum film and the quartz backing material making up the gage. For a constant amplitude heat pulse (Q), Φ is related to the gage response as follows:

$$\Phi = \frac{\Delta E}{\sqrt{t}} \Big/ 2QE_0 \tag{13}$$

The constant amplitude heat-pulse was supplied by joule heating the gage with a constant amplitude current pulse and bridge circuit similar to that described by previous investigators (Ref. 8). The joule heating of the gage is given by

$$Q = \frac{I^2 R}{A} \tag{14}$$

where I is the amplitude of the current pulse, R is the total gage resistance, and A is the measured area of the thin platinum film. An oscillogram of the current pulse and the parabolic gage response is shown in Fig. 8. The time history of the gage output voltage may be measured from the oscillogram and plotted as ΔE vs $\sqrt{t}$ (shown in Fig. 9). The slope of this curve determines $\Delta E/\sqrt{t}$. The current pulse ,I, is measured from the oscillogram and Eq. (14) is used to determine the joule heating. Equation (13) may then be solved for Φ.

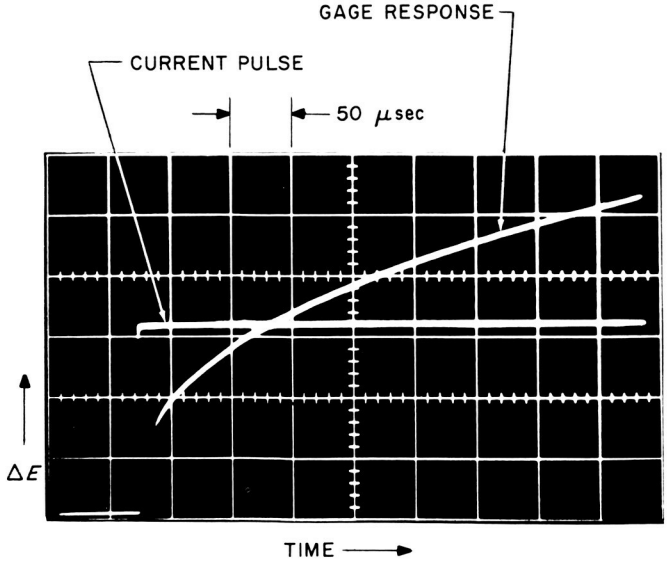

Fig. 8. Oscillogram showing radiation gage response to a constant amplitude heat pulse

For the very high resistance and extremely thin films used in the present investigation (1690 Ω/cm²), the value of Φ was approximately 3×10^{-3} cm²/w$\sqrt{\text{sec}}$. This may be compared with the previously reported (Ref. 8) values of 10^{-2} cm²/w$\sqrt{\text{sec}}$. The previously reported values were in fairly good agreement with the value of Φ calculated using the bulk material and thermal properties of platinum and quartz. By using thicker films of platinum, results agreed with those calculated from the bulk properties. The large differences in Φ due to the film thickness effects indicate that large errors are possible if the direct calibration procedure is not used.

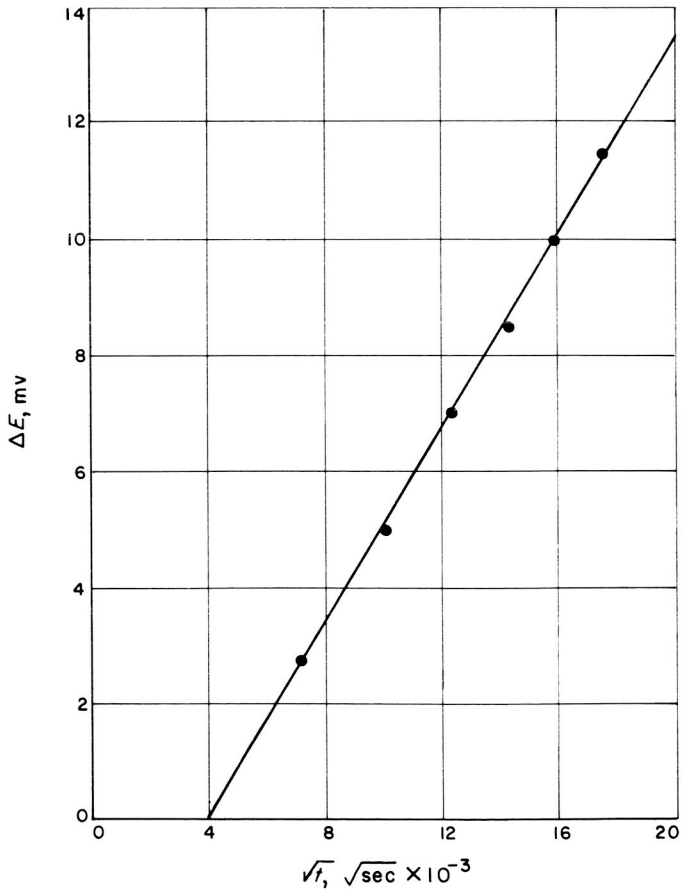

Fig. 9. Typical gage calibration results

V. SHOCK TUBE MEASUREMENTS

The method used to measure the stagnation point heating is illustrated in Fig. 1. A photograph of the shock tube model is presented in Fig. 10. A spider mount was used to support the model coaxially along the shock tube centerline facing the on-coming incident shock wave. After the incident shock passed the model, a bow shock was formed in a few μsec, and a steady constant thickness layer of gas behind the bow shock was viewed by the gage until the test time was terminated by the arrival of the contact surface.

A typical trace of the gage response is presented in Fig. 11. The slight bump on the trace indicates arrival of the incident shock. The formation of the bow shock requires approximately 4 μsec, after which a parabolic response of the gage begins. Also shown in Fig. 11 is the output of a photomultiplier viewing the test gas ahead of the bow shock. Independent measurements of the time required to form the bow shock under the same shock tube conditions using collimated photomultipliers

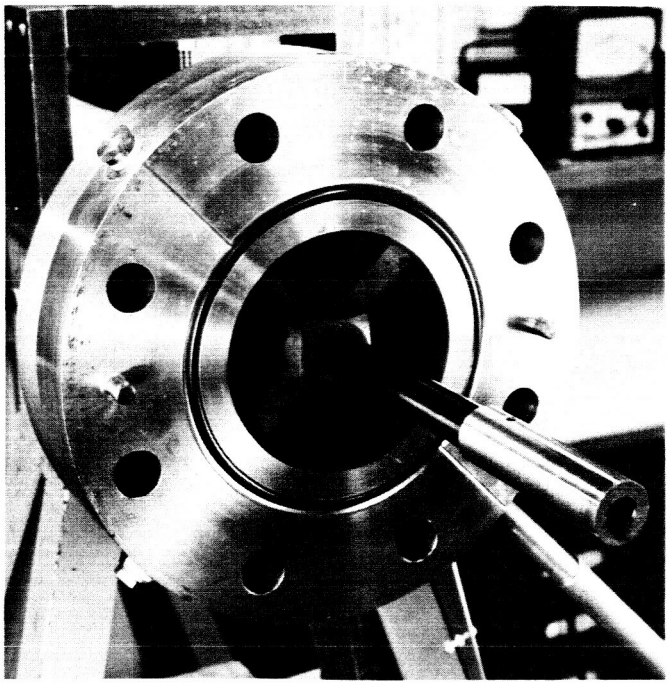

Fig. 10. Photograph of the shock tube model used for stagnation point radiative heat transfer measurements

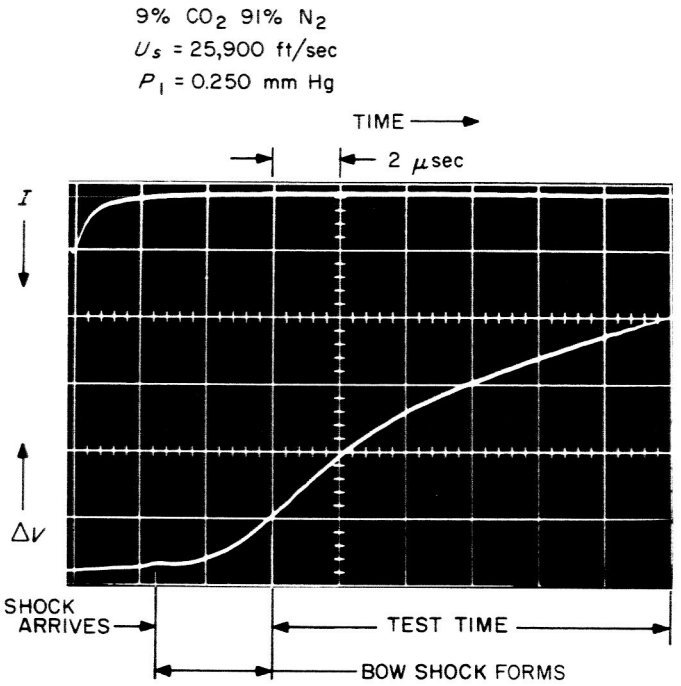

Fig. 11. Oscilloscope trace showing response of the stagnation point total radiation gage

indicated approximately 2 to 3 μsec for the formation time. Therefore, the gage response time is on the order of 1 or 2 μsec, which agrees with the previous theoretical estimate. Preliminary measurements of the total radiation from a shock heated mixture of 9% CO_2-91% N_2 are presented in Fig. 12. This mixture was chosen to simulate a possible composition of the atmosphere of the planet Venus. The results are compared with some recent equilibrium calculations for a mixture of 7.5% CO_2-92.5% N_2 and also with the free flight data of James (Ref. 9) for a mixture of 9% CO_2-91% N_2. The calculated curves for various free-stream pressures are correlated by normalizing the results with a suitable power of the stagnation pressure.

As may be seen in Fig. 12, the experimental data are in good agreement with both the calculated and experimental results above 25,000 ft/sec. On the basis of these results, it appears that the total radiation heat transfer gage provides a useful and reliable technique for measuring the radiation from high-temperature gases.

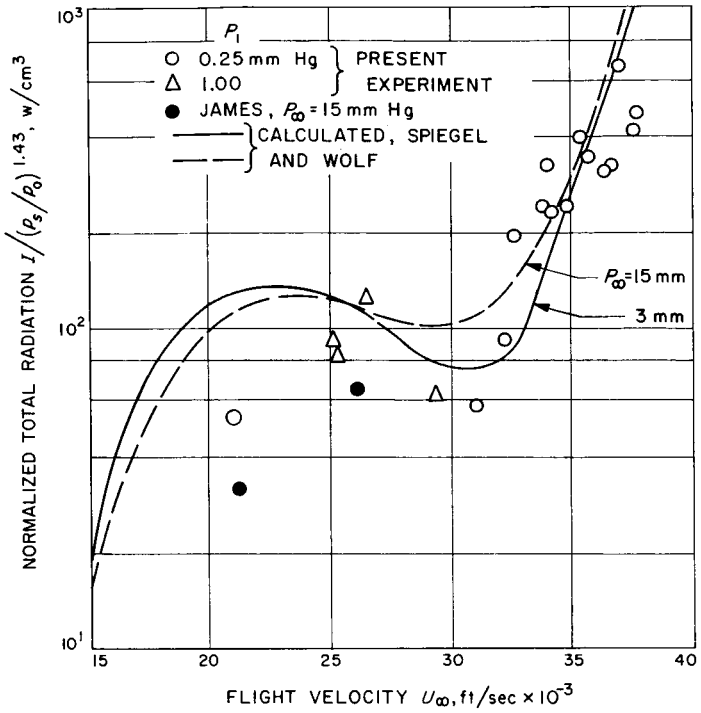

Fig. 12. Normalized stagnation point total radiation for a mixture of 9% CO_2-91% N_2 compared with free flight experimental data and equilibrium calculations

NOMENCLATURE

A	area of gage element
C	heat capacity
E, V	gage potential
F	fraction of incident intensity absorbed by carbon film
$f(y)$	$= \int \frac{dV \cos\theta}{S^2}$ view factor
$\bar{G}$	total or integrated radiance
G_λ	spectral radiance
I	gage current
k	thermal conductivity
L	length of gage element
l	thickness of carbon film
p	pressure
Q	constant heat input
$q(t)$	arbitrary, time-dependent heat input
R	gage resistance
r	resistance per unit length
s	distance from differential gage element to volume element
T	temperature of platinum film
T^*	asymptotic temperature of carbon-P_t interface
t	time
U	fraction of incident intensity reflected from carbon film
V	gas volume
W, I	gas radiance, w/cm³
x	distance normal to gage surface
y	distance along gage surface
α	temperature coefficient of resistance

β thermal and material property of quartz $= \sqrt{\pi \rho_2 C_2 k_2}$

δ thickness of plane parallel layer

θ angle between vector normal to gage surface and vector from gage element to volume element

λ wavelength

$\mu_{\lambda 0}$ spectral transmission of window

$\xi = L\pi/\mu_{\lambda 0} F E_{\lambda 0} \Phi \int f_i(y)dy$

ρ mass density

σ $\sqrt{\rho_2 C_2 k_2 / \rho_1 C_1 k_1}$

τ thermal transit time

$\Phi = \alpha/\beta$

Subscripts

1 Material 1 (also initial driven gas conditions)

2 Material 2

g gage

i ith area element

0 initial condition of gage at temperature T_0 and current I_0 (also STP reference conditions)

s stagnation conditions

w window

λ wavelength dependent quantities

∞ free-stream conditions (also flight conditions)

REFERENCES

1. Rabinowicz, J., Jessey, M. E., and Bartsch, C. A., Resistance Thermometer for Heat *Transfer Measurements in a Shock Tube*, Galcit Memo No. 33, July, 1956.
2. Hall, G. J., and Hertzberg, A., "Recent Advances in Transient Surface Temperature Thermometry," *Jet Propulsion*, pp. 719–723, November, 1958.
3. Gruszczynski, J. S., Harris, C. J., Rodgers, D. A., and Warren, W. R. Jr., *Fast Response Total Radiation Gage for Measurement of Radiant Emission from High Temperature Gas*, IEEE Paper No. 63–438, January, 1963.
4. Hoshizaki, H., *Equilibrium Total Radiation Measurements in Air at Superorbital Entry Velocities*, Third Hypervelocity Techniques Symposium, University of Denver, Denver, Colorado, March 17–18, 1964.
5. Camac, M., and Feinberg, R., *High Speed Infrared Bolometer*, Avco Everett R.R. 120, March, 1962.
6. Valasek, J., "Optical Constants of Substances Which Exhibit Metallic Reflection," International Critical Tables, Vol. V, 1929.
7. Kivel, B., *Radiation from Hot Air and Stagnation Heating*, Avco Everett R.R. 79, October, 1959.
8. Hewitt, E. W., *Description of the Aeromechanics Laboratory Heat Transfer Gage Calibration Unit*, Space Technology Laboratories, STL/TN-60-0000-19200, November, 1960.
9. James, Carlton S., *Experimental Study of Radiative Transport From Hot Gases Simulating in Composition the Atmospheres of Mars and Venus*, AIAA Paper No. 63–455, August, 1963.

APPENDIX

View Factor for Plane Parallel Layer

It is necessary to determine the integrated view factor term for the experimental geometry illustrated in Fig. A-1. The gage views the radiation from a plane parallel shock layer of thickness δ through a hole of radius a. The view factor was defined previously as

$$f_i(y) = \int \frac{dV \cos\theta}{S_i^2} \tag{A-1}$$

In order to simplify the calculation, the shock layer was divided into N slices. The case $N = 2$ is illustrated in Fig. A-1. The truncated oblique cone is approximated by cylinder sections of thickness Δx. As can be seen from the geometry, the radius of the jth slice is given by

$$a_j = a_1 \frac{b_j}{b_1} \qquad j = 1 \rightarrow N \tag{A-2}$$

while the vertical distance of the jth cylinder base above the element area dA_i is given by

$$b_j = b_1 + (N_j - 1)\,\Delta x \tag{A-3}$$

where $N_j = j$th slice.

The contribution of the jth slice to the view factor of the elemental area dA_i is independent of the other slices and is given by

$$f_{ij} = \int \frac{dV \cos\theta}{S_{ij}^2} \tag{A-2}$$

The view factor for dA_i is therefore given by the sum of the contributions from all slices.

$$f_i = \sum_{j=1}^{N} f_{ij} \tag{A-3}$$

For the geometry of Fig. A-1,

$$f_{ij} = 2b\Delta x \int_{-\pi/2}^{\pi/2} \int_0^a \frac{r'dr'd\beta'}{(c^2 + 2cr' \sin\beta' + r'^2 + b^2)^{3/2}} \tag{A-4}$$

which may be written

$$\frac{f_{ij}}{2b\Delta x} = \frac{a^2}{c^3} \int_0^{\pi} \int_0^1 \frac{rdrd\beta}{[1 + 2Ar\cos\beta + A^2r^2 + B^2]^{3/2}} \tag{A-5}$$

where

$$r = \frac{r'}{a} \qquad A = \frac{a}{c} \qquad B = \frac{b}{c} \qquad \beta = \frac{\pi}{2} - \beta'$$

Since r' is not β' dependent, Eq. (A-5) may be written

$$\frac{f_{ij}}{2b\Delta x} = \frac{a^2}{c^3} \int_0^1 \frac{rdr\,E_1(r)}{[1 + A^2r^2 + B^2]^{3/2}} \tag{A-6}$$

where

$$E_1(r) = \int_0^{\pi} \frac{d\beta}{[1 + Z\cos\beta]^{3/2}} \tag{A-7}$$

and

$$Z = \frac{2Ar}{[1 + A^2r^2 + B^2]}$$

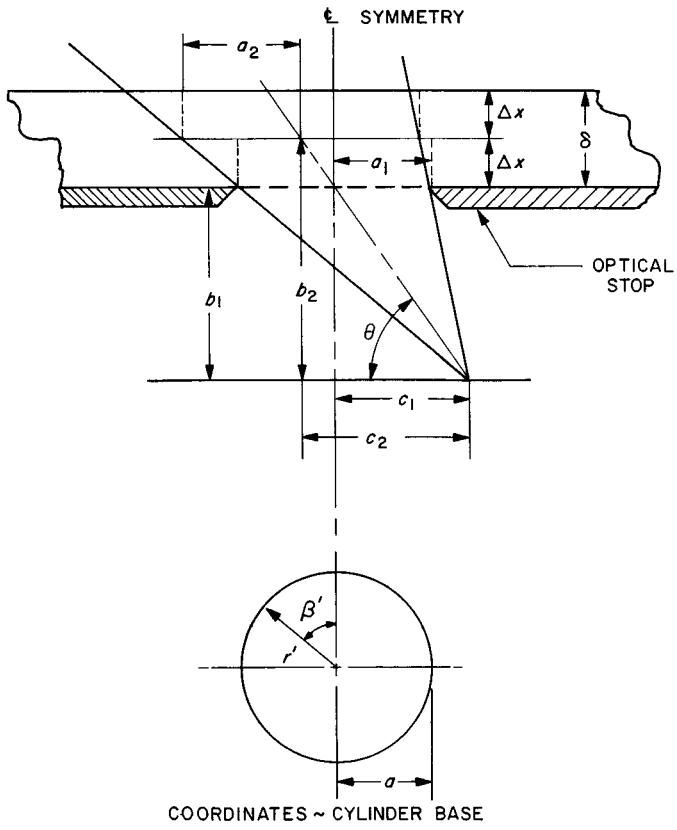

Fig. A-1. Geometry for approximate solution of the view factor for a plane parallel layer

Using standard integration formula, Eq. (A-7) may be written in the form

$$E_1(r) = \frac{1}{1 - Z^2}\int_0^{\pi} (1 + Z\cos\beta)^{1/2}\, d\beta$$

Expanding this expression in power series, the following result is obtained:

$$E_1(r) = \pi\left(1 + \tfrac{15}{16} Z^2 + \frac{2835}{3072} Z^4 + \cdots\right) \tag{A-8}$$

This series converges for $Z \leqq 1$. The number of terms which must be retained for an accurate approximation may be estimated as follows: From the actual experimental geometry,

$$A = 1/2 \qquad B = 2.0 \qquad 0 \leqq r \leqq 1$$

Therefore,

$$Z = \frac{2Ar}{(1 + A^2r^2 + B^2)} = \frac{r}{\left(5 + \frac{r^2}{4}\right)}$$

The worse case for convergence is clearly $r' = 1.0$, which gives $Z \approx \frac{1}{4}$. This value of Z, when substituted in Eq. (A-8), gives

$$E_1(r) = \pi\left[1 + \underset{0.0585}{0(Z^2)} + \underset{0.0039}{0(Z^4)} + \cdots\right]$$

The error in neglecting terms of $0(Z^4)$ is less than ½%, and the expression for $E_1(r)$ was taken to be

$$E_1(r) = \pi\left[1 + \tfrac{15}{16} Z^2\right] \tag{A-9}$$

Substituting (A-9) in (A-6),

$$\frac{f_{ij}}{2b\Delta x} = \frac{\pi a^2}{c^3}\left(\frac{E_2(q)}{(1 + B^2)^{3/2}} + \frac{15}{4}\frac{A^2E_3(q)}{(1 + B^2)^{7/2}}\right) \tag{A-10}$$

$$E_2(q) = \int_0^1 \frac{r\,dr}{(1 + qr^2)^{3/2}} \tag{A-11}$$

$$E_3(q) = \int_0^1 \frac{r^3\,dr}{(1 + qr^2)^{7/2}} \tag{A-12}$$

where

$$q = \frac{A^2}{1 + B^2}$$

The integral of Eq. (A-11) may be found in standard integral tables and the result is

$$E_2(q) = \frac{1}{q}\left(1 - \frac{1}{\sqrt{1 + q}}\right) \tag{A-13}$$

Using repeated integration by parts gives the result

$$E_3(q) = \frac{1}{q}\left[\frac{\sqrt{1 + q}}{3q(1 + q)^2} - \frac{8}{15q} + \frac{\sqrt{1 + q}}{5q(1 + q)^3} + \frac{4}{15\sqrt{1 + q}}\left(2 + \frac{1}{1 + q}\right)\right] \tag{A-14}$$

Substituting Eqs. (A-13) and (A-14) in Eq. (A-10), the solution for the view factor is

$$f_{ij} = \frac{2b\Delta x\pi a^2}{c^3 q(1 + B^2)^{3/2}}\left\{\left(1 - \frac{1}{\sqrt{1 + q}}\right) + \frac{15}{4}\frac{A^2}{(1 + B^2)^2}\left[\frac{\sqrt{1 + q}}{3q(1 + q)^2} - \frac{8}{15q} + \frac{\sqrt{1 + q}}{5q(1 + q)^3} + \frac{4}{15\sqrt{1 + q}}\left(2 + \frac{1}{1 + q}\right)\right]\right\} \tag{A-15}$$

As a check on the result, it is noted that for the special case $c = 0$, Eq. (A-4) becomes

$$\frac{f_{ij}}{2b\Delta x} = \int_{-\pi/2}^{\pi/2}\int_0^a \frac{r'dr'd\beta}{(r'^2 + b^2)^{3/2}} \qquad c = 0$$

This expression can be integrated exactly to give

$$\frac{f_{ij}}{2b\Delta x} = \pi\left(\frac{1}{b} - \frac{1}{\sqrt{a^2 + b^2}}\right) \tag{A-16}$$

Now, the limit of Eq. (A-10) is taken as $c \to 0$. The second term in the brackets is zero since

$$\lim_{c \to 0} \frac{A^2}{(1 + B^2)^{7/2}} = 0$$

and Eq. (A-10) becomes

$$\frac{f_{ij}}{2b\Delta x} = \frac{\pi a^2 E_2(q)}{c^3(1 + B^2)^{3/2}}$$

Noting that

$$\lim_{c \to 0} q = \left(\frac{a}{b}\right)^2$$

$$\lim_{c \to 0} E_2(q) = \left(\frac{b}{a}\right)^2\left[1 - \frac{b}{\sqrt{a^2 + b^2}}\right]$$

$$\lim_{c \to 0} \frac{\pi a^2}{c^3(1 + B^2)^{3/2}} = \frac{\pi a^2}{b^3}$$

the result is

$$\lim_{c \to 0} \frac{f_{ij}}{2b\Delta x} = \pi \left(\frac{1}{b} - \frac{1}{\sqrt{a^2 + b^2}} \right)$$

which is identical with the exact solution in Eq. (A-16).

Equation (A-15) was solved for the view factor $f_i(y)$ for the particular geometry of the experiment. The results are presented in nondimensional form in Fig. A-2. A single-step calculation with $\Delta x = \delta$ gave results accurate to 1% for small stand-off distances ($\delta \leqq 10$ mm) using the particular geometry chosen here. The view factor is symmetric about the centerline of the gage and has its maximum value at the centerline ($c = 0$). At the edge of the gage ($c/y_0 = 1.0$), the view factor falls to less than 50% of the maximum value. The integrated view factor $\int_0^{y_0} f_i(y)dy$ may be obtained from the area under the curve in Fig. A-2.

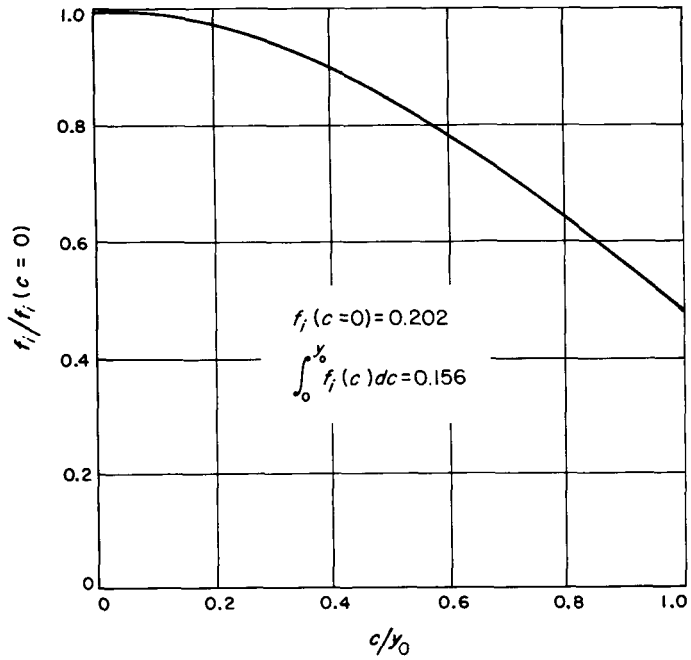

Fig. A-2. View factor for the experimental geometry: a = 0.795 cm; b = 2.11 cm; and y_0 = 0.953 cm

ACKNOWLEDGMENTS

The authors are indebted to the following personnel at JPL for various phases of this work: Terry Babineaux, Clarence Tuttle, and Robert H. Lee for the shock tube experiments; David Etheridge for construction of the gages; and Ray Hill for the development of the pulse circuit for gage calibration.